1 Red and black: A β-carotene-binding protein carrying a red pigment

2 regulates body-color transition in locusts

3 **Meiling Yang[1‡], Yanli Wang[2‡], Qing Liu[1‡], Zhikang Liu[1], Feng Jiang[3], Huimin**

4 **Wang[3], Xiaojiao Guo[1], Jianzhen Zhang[2*], Le Kang[1,3*]**

5 [1]State Key Laboratory of Integrated Management of Pest Insects and Rodents,

6 Institute of Zoology, Chinese Academy of Sciences, Beijing 100101, China

7 [2]Institute of Applied Biology, Shanxi University, Taiyuan 030006, Shanxi, China

8 [3]Beijing Institutes of Life Science, Chinese Academy of Sciences, Beijing

9 100101, China

10 **Running head: βCBP regulates the body color change of locusts**

11 **‡ These authors contributed equally to this study.**

12 *** Corresponding author**

13 Le Kang, Ph.D. and Professor

14 Institute of Zoology, Chinese Academy of Sciences

15 Beijing 100101, China

16 Tel.: 86-10-6480-7219

17 Fax: 86-10-6480-7099

18 E-mail: lkang@ioz.ac.cn

19

20

Abstract

21

22   Changes of body color have important effects for animals in adapting to

23 variable environments. The migratory locust exhibits body color polyphenism

24 between solitary and gregarious individuals, with the former displaying a

25 uniform green coloration and the latter having a prominent pattern of black

26 dorsal and brown ventral surface. However, the molecular mechanism

27 underlying the density-dependent body color changes of conspecific locusts

28 remain largely unknown. Here, we found that up regulation of β-carotene-

29 binding protein promotes the accumulation of red pigment, which added to the

30 green color palette present in solitary locusts changes it from green to black,

31 and that down regulation of this protein led to the reverse, changing the color

32 of gregarious locusts from black to green. Our results provide insight that color

33 changes of locusts are dependent on variation in the red β-carotene pigment

34 binding to βCBP. This finding of animal coloration corresponds with trichromatic

35 theory of color vision.

36 **Introduction**

37 Body color change is a ubiquitous but highly diverse phenomenon of adaptive

38 significance to animals under exposure to illnesses, environmental changes,

39 predation, and sexual signals (*Burmeister et al.*, *2005; Henderson et al.*, *2016;*

40 *Mathger*, *2003; Stuart-Fox and Moussalli*, *2008; Teyssier et al.*, *2015*).

41 Seasonal switching between color phases in response to extrinsic

42 environmental factors is common in arthropods (*Futahashi and Fujiwara*, *2008;*

2

43 *Futahashi et al., 2012; Moran and Jarvik, 2010*). However, rapid and reversible

44 color change is a rare trait regulated by endogenous and exogenous

45 mechanisms (*Cuthill et al., 2017; Hubbard et al., 2010*). This type of phenotypic

46 plasticity has not been well investigated.

47 Rapid body color change in arthropods such as aphids, locusts and

48 grasshoppers, lepidopteran caterpillars, and spider mites is influenced by

49 environmental changes, especially by changes in population density (*Bryon et*

50 *al., 2017; Tabadkani et al., 2013; Valverde and Schielzeth, 2015; Wang and*

51 *Kang, 2014; Xiong et al., 2017*). Locust body color changes are of particular

52 interest because conspecific color change coincides with changes in population

53 density as well as behavioral changes; specifically, dramatic individual color

54 change from green to black occurs when locusts form agriculturally destructive

55 swarms (*X. Wang et al., 2014; Wang and Kang, 2014; Wu et al., 2012b*). Similar

56 to that of other animals (*Cuthill et al., 2017; Duarte et al., 2017*), the coloration

57 of locusts serves as a dynamic form of population information.

58 Phenotypic plasticity in the migratory locust *Locusta migratoria* underlies

59 the transition between the gregarious and solitary phases, which are dependent

60 on population density changes (*Guo et al., 2011; Kang et al., 2004; Ma et al.,*

61 *2011; Wu et al., 2012a; Yang et al., 2014*). In addition to behavioral differences

62 between the two phases of locusts (*Kang et al., 2004; Ma et al., 2011; Yang et*

63 *al., 2014*), remarkable body color changes between gregarious and solitary

64 locusts occur. Solitary locusts found at low population densities have a uniform

65   green coloration, whereas gregarious locusts develop a striking color pattern of

66   a black back with a contrasting brown ventral color (*Pener, 1991; Wang and*

67   *Kang, 2014*).

68   The black-brown pattern of gregarious locusts is recognized as mainly

69   being induced under high-density crowding conditions (*Pener, 1991*).

70   Regarding the regulatory mechanism, juvenile hormones reportedly induce

71   solitary green cuticular coloration in locusts (*Applebaum et al., 1997; Tanaka,*

72   *1993*). However, the regulatory function of these hormones during phase

73   change remains controversial (*Wang and Kang, 2014*). The neuropeptide

74   [His7]-corazonin induces a dark coloration of the whole body in locusts but does

75   not regulate the phase-related black–brown color pattern in gregarious locusts

76   (*Tanaka, 2000; Wang and Kang, 2014*). Silencing the *ebony* and *pale* genes in

77   the dopamine pathway that leads to the synthesis of dopamine melanin can

78   result in partial fading of the black color in gregarious locusts, but the

79   exogenous injection of dopamine does not completely lead to the black pattern

80   (*Ma et al., 2011*). Thus, the body color pattern of gregarious locusts is not the

81   result of pure melanization.

82   The green color of solitary locusts is likely due to the presence of a

83   combination of yellow and blue pigments (*Pener and Simpson, 2009*) that

84   facilitate the camouflage of low-density locusts in the background of plants. In

85   the present study, we investigated whether the black coloration of gregarious

86   locusts results from the addition of pigments to the solitary green background.

4

87   We used strand-specific high-throughput RNA sequencing to monitor

88   genome-wide transcriptional expression profiles and detect differentially

89   expressed genes (DEGs) correlated with color polymorphism. We found a key

90   DEG that encodes β-carotene-binding protein (βCBP), which promotes body

91   color change associated with phase-related coloration. The manipulation of the

92   gene expression by RNAi and feeding of β-carotene led to the reverse of body

93   color of the locusts. The results of our study reveal that the black–brown

94   coloration pattern in gregarious locusts is formed by the presence of the red

95   color β-carotene pigment–βCBP protein complex in the green-colored

96   background of solitary locusts. This work provides novel insights into the

97   molecular mechanisms of body color changes in response to population density

98   changes in accordance with the corresponding environmental changes.

99   **Results**

100   **Gregarious and solitary locusts have different expression levels of βCBP**

101   Gregarious and solitary locusts were reared either in crowded conditions or in

102   solitude as previously described (*Ma et al.*, *2011*). These locusts displayed

103   phase-specific phenotypes of body coloration. The gregarious locusts exhibited

104   intense black patterns with a ventral brown color, and the solitary locusts

105   showed the expected uniform green coloration (*Figure 1A*).

106   The body coloration of gregarious locusts is characterized as a black

107   tergum of the thorax and abdomen, in particular, a very black pronotum. To

108   delineate gene activity changes potentially associated with the regulation of

109   phase-dependent body color traits, we performed transcriptome sequencing on

110   pronotum integuments of gregarious and solitary locusts. We identified a total

111   of 1653 DEGs between the gregarious and solitary locusts (*Figure 1―figure*

112   *supplementary 1A*), and 26% (430) of these DEGs were protein-coding genes

113   (*Figure 1―figure supplementary 1B*). Gene ontology analysis of these 430

114   protein-coding DEGs indicated that many of them encode cuticle metabolism-

115   related proteins involved in chitin metabolic, melatonin metabolic, transport,

116   and catecholamine catabolic activities (*Figure 1―figure supplementary 1C*).

117   Sixty-eight of the 430 protein-coding DEGs are involved in pathways

118   associated with animal coloration (*Figure 1B*). The top 17 DEGs (Log FC > 2.8,

119   FDR < 1e-5) of these 68 genes were used to validate the differential expression

120   patterns between the gregarious and solitary locusts via qPCR (*Figure 1C*).

121   Nine of the 17 genes showed higher transcriptional levels in the pronotum

122   integuments of the gregarious locusts than in those of the solitary locusts, and

123   the transcriptional levels of 6 of the 17 genes were significantly lower in the

124   gregarious locusts than in the solitary locusts (*Figure 1C*). These results are

125   consistent with the transcriptome data. Among the 17 genes, we investigated

126   the top 8 DEGs, among which 6 had higher expression in the gregarious locusts

127   and 2 had higher expression in the solitary locusts, to screen the key candidate

128   genes involved in the color change.

129   To explore whether these 8 genes regulate body color plasticity during

130   locust phase transition, we carried out transcript knockdown analyses of these

6

131 genes in the gregarious and solitary locusts. Out of the 8 genes, only *βCBP*

132 showed a significant effect on the regulation of body color transition when it was

133 silenced. After molting, the dark pattern in the pronotum decreased markedly in

134 60% of the gregarious locusts after *βCBP* knockdown (*Figure 1 —figure*

135 *supplementary 2*). These data imply that *CBP* serves as a key gene involved in

136 body color change.

137 **Phase-related characteristics of the *βCBP* gene in integument**

138 To investigate the correlation of βCBP expression level with the degree of black

139 body coloration of the locust integument, we performed quantitative reverse

140 transcriptase–polymerase chain reaction (qRT–PCR) and found that *βCBP* was

141 predominantly expressed in the locust integument tissue (*Figure 2 —figure*

142 *supplementary 1*). Furthermore, consistent with the deeper black color of the

143 pronotum than of the tergum of the thorax and abdomen in gregarious locusts,

144 we found that *βCBP* expression was significantly higher in the pronotum than

145 in the tergum integuments of the thorax and abdomen in gregarious locusts,

146 whereas little *βCBP* expression was observed in the terga of solitary locusts,

147 with no variability among the tergum segments (*Figure 2A*). Because the black

148 coloration of gregarious locusts gradually increases with nymph developmental

149 stage, we also quantified the *βCBP* transcript levels in the pronotum of different

150 developmental stages of the gregarious locusts. The *βCBP* transcript level

151 increased with developmental stage, with the expression levels of 4th instar

152 gregarious locusts being approximately 200 times those of the 2nd and 3rd instar

153   gregarious locusts. By contrast, βCBP expression was invariable across the

154   developmental stages in solitary locusts (*Figure 2B*). Therefore, the extent of

155   black body coloration in locusts is positively correlated with *βCBP* expression

156   level.

157   To explore whether βCBP is especially expressed in the black tergum

158   integuments of gregarious locusts, we performed a comparative analysis via

159   qRT–PCR to quantify the *βCBP* transcript levels in the tergum integuments of

160   solitary and gregarious locusts. The transcript level of *βCBP* was significantly

161   higher in the pronotum and tergum integuments of the thorax and abdomen of

162   gregarious individuals than the pronotum and tergum integuments of solitary

163   individuals (*Figure 2C* and *Figure 2―figure supplementary 3*). Moreover,

164   isolating the gregarious locusts (IG) significantly decreased the transcript level

165   of *βCBP* (*Figure 2C* and *Figure 2―figure supplementary 2, 3*). By contrast,

166   crowding the solitary locusts (CS) significantly increased the transcript level of

167   *βCBP* (Figure 2*C* and *Figure 2―figure supplementary 3*).

168   Because the expression pattern of *βCBP* in the pronotum was consistent

169   with that in the tergum of the thorax and abdomen, the pronota were considered

170   representative of all terga of locusts in the following analyses. We also found

171   that the level of CBP protein in the locust pronotum integuments was

172   significantly higher in the gregarious locusts than in the solitary locusts

173   (*Figure 2D*). Moreover, the protein levels of βCBP declined when the locusts

174   were isolated and increased under the crowding conditions (*Figure 2D*). This

175   expression pattern suggests a potential role of βCBP in regulating the body

176   color characteristics of the pronotum and tergum integuments of the thorax and

177   abdomen.

178   To determine whether βCBP is differentially localized in the locust

179   pronotum integuments of gregarious and solitary locusts, we performed

180   immunohistochemistry of βCBP. We found that large amounts of βCBP were

181   widely detected in the intercellular space of the pronotum of gregarious locusts,

182   whereas βCBP was distributed very sporadically in the solitary locusts

183   (*Figure 2E*). The amount of βCBP protein in the pronotum of gregarious locusts

184   was 39.5-fold higher than the corresponding amount in solitary locusts (*Figure*

185   *2G*). Furthermore, the amount of βCBP protein in the locust pronotum was

186   decreased by isolation and increased by crowding (*Figure 2F and G*).

187   Considering that βCBP can bind and accumulate β-carotenes in tissues

188   (*Bhosale and Bernstein, 2007*), we assessed the amount of β-carotene binding

189   by βCBP in the pronotum integuments of gregarious and solitary locusts in vivo.

190   The β-carotene content in the gregarious locusts was 2.8-fold higher than that

191   in the solitary locusts (*Figure 2H*). These results suggest that βCBP protein

192   level and the associated β-carotene content are directly correlated with the

193   degree of black coloration of the locust pronotum.

194   **βCBP mediates body color changes associated with population density**

195   Based on the high level of βCBP available to bind with β-carotenes in

196   gregarious locusts or crowded solitary locusts, we hypothesized that the black

197 gregarious locusts could be induced towards green body color by blocking

198 βCBP synthesis to interfere with β-carotene deposition. To confirm the

199 involvement of βCBP in pigmentation during the phase transition, we injected

200 double-stranded RNAs (dsRNAs) against the *βCBP* gene into the abdominal

201 hemocoel of gregarious nymphs at the second stadium, isolated the injected

202 locusts, and assessed their body color pattern.

203   After injection of *dsβCBP*–RNA and isolation treatment, the mRNA and

204 protein levels of βCBP in the pronotum integument decreased by 99% and 85%,

205 respectively, relative to the levels in *dsGFP*–RNA-injected and isolated controls

206 (*Figure 3A and C*). In addition, the mRNA levels of *βCBP* in the tergum of the

207 thorax and abdomen decreased by 98% relative to the levels in *dsGFP*–RNA-

208 injected and isolated controls (*Figure 3—figure supplement 1*). The silencing

209 effect of *dsβCBP*–RNA resulted in an 80% decrease in the signal intensity of

210 βCBP in the pronotum integuments of gregarious locusts relative to the

211 corresponding intensity in the *dsGFP*–RNA injected controls (*Figure 3E and F*).

212   We then determined the effects of *βCBP* silencing on the β-carotene

213 content in the pronotum integuments of locusts. Because there are many free

214 β-carotenes in locusts and β-carotene only binds with the βCBP protein to

215 participate in the formation of body color, we measured the amount of β-

216 carotene binding to βCBP. The administration of *dsβCBP* significantly reduced

217 the β-carotene content in the pronotum integuments from 104.8 ug/g to 74.3

218 ug/g (*Figure 3H*).

219   A body coloration assay revealed that after molting of 29 locusts, 48% of

220   the nymphs injected with dsβCBP–RNA and then isolated showed substantial

221   lightening of the black pronotum. Moreover, 41% of the gregarious nymphs

222   shifted to a complete green-colored body. By contrast, 73% of the *dsGFP–*

223   RNA-injected gregarious nymphs treated with isolation retained an intense

224   black body pattern. Only 27% of the *dsGFP*-injected and isolated control locusts

225   showed body color lightening (*Figure 4A*). These results support the view that

226   βCBP regulates the body color changes of gregarious and solitary locusts

227   between black and green coloration.

228   To further confirm the direct involvement of βCBP in mediating body color

229   changes, we assessed the effect of increasing the pigment bound with βCBP

230   on the body color change of locusts from solitary to gregarious phase. In this

231   experiment, solitary locusts were fed a diet containing β-carotene and treated

232   with crowding. The mRNA and protein levels of βCBP significantly increased

233   by 11.2- and 2.5-fold in the pronotum, respectively, and increased by 2.3- and

234   2.1-fold in the tergum of the thorax and abdomen, respectively, relative to the

235   corresponding levels in the regular diet-fed and crowded controls (Figure 3*B, D*

236   and *Figure 3—figure supplement 2*). Moreover, the signal intensity of βCBP

237   increased by 22.7-fold in the pronotum integument cells of the solitary locusts

238   after β-carotene feeding and crowding relative to the intensity in the regular

239   diet-fed and crowded controls (*Figure 3E and G*). In addition, HPLC analysis

240   revealed that the amount of βCBP–β-carotene complex in the solitary

11

241 integuments increased by 3.4-fold after β-carotene feeding and crowding

242 (*Figure 3H*). A total of 47% of the solitary locusts completely shifted to the

243 typical gregarious body color, and the pronota of 33% of the feeding locusts

244 developed extensive black areas similar to the gregarious body color after

245 feeding with β-carotene and crowding. However, 87% of the locusts retained

246 their green color in the regular diet and crowding treatment (control group)

247 (*Figure 4B*). Thus, βCBP and β-carotene can jointly induce body color changes

248 from green to black associated with phase transition in locusts.

249   To further determine whether the βCBP upregulation induced by β-

250 carotene is responsible for the body color change of locusts from green to black,

251 we conducted a rescue experiment by injecting *dsβCBP*-RNA into solitary

252 locusts pre-fed with β-carotene. After molting, 35.5% of the *dsβCBP*-injected

253 nymphs pre-fed with β-carotene showed green body color, whereas 15.6% of

254 the green individuals in the *dsGFP*-injected group pre-fed with β-carotene did

255 so. Correspondingly, the phenotype of black tergum individuals induced by β-

256 carotene was rescued only by injection with *dsβCBP*-RNA (*Figure 4C*).

257 Therefore, βCBP acts with β-carotene to regulate the black body color of

258 gregarious locusts.

259 **Body color change from green to black is mediated by the red pigment**

260 **complex**

261 To confirm the role of the βCBP–pigment complex in black color pigmentation,

262 we performed a pigment immunoprecipitation assay using an antibody against

12

263   the βCBP protein in vitro and in vivo to examine the binding capacity and

264   complex coloration of βCBP with β-carotene (*Figure 5A and B*). We incubated

265   recombinant βCBP (rβCBP) with β-carotene under immunoprecipitation by

266   using βCBP antibody conjugated with protein A-Sepharose (*Figure 5A*).

267   Immunoprecipitation of β-carotene-rβCBP formed a red complex, whereas no

268   red precipitate formed when β-carotene was added to bovine serum albumin

269   (BSA) or when β-carotene in the absence of rβCBP was incubated in the

270   binding buffer followed by immunoprecipitation (*Figure 5A*). It could be inferred

271   that the red precipitate was specific to the rβCBP–β-carotene complex because

272   this complex failed to form in the presence of BSA and β-carotene or in the

273   absence of rβCBP (*Figure 5A*). The pigment immunoprecipitation assay in vivo

274   also showed an accumulation of red pigment in the precipitate of the integument

275   when treated with anti-βCBP-immunoprecipitation compared with IgG-

276   immunoprecipitation (*Figure 5B*). Furthermore, we confirmed that the red

277   pigment in the βCBP precipitant result from β-carotene by HPLC analysis

278   (*Figure 5—Figure supplement 1*). These results provide strong evidence that

279   βCBP directly binds with β-carotene in the pronotum integument to form the red

280   complex, which directly contributes to the black pattern of the pronotum in

281   gregarious locusts.

282   **βCBP is localized to the pigment granules of the pronotum integument**

283   To verify the co-location of βCBP and the pigment granules, we investigated

284   the subcellular distribution of βCBP using immunoelectron microscopy. The

13

285 pronotum integuments were fixed and embedded for thin sections. The sections

286 were analyzed for βCBP localization by using an anti-βCBP antibody followed

287 by a gold-conjugated antibody against rabbit IgG. The gold particles were

288 present mainly in the pigment granules of the pronotum integuments. In addition,

289 the average number of gold particles in the pigment granules from the pronotum

290 integuments was 15.5-fold higher in the gregarious locusts than in the solitary

291 locusts (*Figure 5C and F*). Furthermore, *βCBP* silencing coupled with isolation

292 caused a severe deficiency of gold particles in the pigment granules of the

293 gregarious locusts, indicating a substantial reduction in the βCBP protein–

294 pigment complex relative to the level in the *dsGFP*-injected and isolated

295 controls (*Figure 5D and G*). By contrast, β-carotene intake coupled with

296 crowding evidently increased the gold particles responsible for the βCBP

297 production in the pigment granules of pronotum in the solitary locusts,

298 demonstrating a significant promotion of βCBP protein–pigment complex

299 accumulation compared with accumulation in the regular diet-fed and crowded

300 controls (*Figure 5E and H*). Thus, the βCBP–pigment complex is a key mediator

301 of black formation in the pronotum integuments of gregarious locusts.

302 **Discussion**

303   Our study revealed an undescribed mechanism of body color regulation in

304 which changes in the βCBP–β-carotene complex-mediated red color balance

305 produce a shift between black and green body color in locusts. The change of

306 body color occurs as an adaptive response to population density change. The

14

307 black–brown pattern in the gregarious locusts resulted from the superposition

308 or balancing effect of a red pigment on the green background of solitary locusts

309 rather than complete melanogenesis. Crowding treatment increased the βCBP

310 levels in the integuments and caused body color change in the solitary locusts

311 by the binding of βCBP with β-carotenes (*Figure 6*). This finding of animal

312 coloration corresponds precisely with the physically trichromatic rule.

313 We demonstrated that βCBP expression is not only positively correlated

314 with the black color of the pronotum in gregarious locusts but also phase-related

315 in response to population density changes. The βCBP expression in solitary

316 locusts was not induced by merely feeding with β-carotene without crowding

317 treatment (*Figure 3—figure supplement 3*). Thus, the body color changes of

318 solitary locusts that were induced to form gregarious-like body coloration must

319 rely on crowding treatment and feeding the β-carotene, because only crowding

320 treatment can promote the βCBP expression for βCBP–β-carotene complex

321 production. Thus, population density of locusts acts as necessary and sufficient

322 condition to drive the changes of body coloration. Generally, body color

323 changes are driven by gene changes to adapt with a broad range of

324 environments. For instance, the melanocortin-1 receptor gene regulates

325 melanin production associated with black hair and skin in human and mouse

326 pigmentation responsed to ultraviolet-light (*D'Orazio et al., 2006*). The

327 cytochrome P450 gene may encode ketolases that generate red carotenes, as

328 a honest signaling, to control the bright-red coloration of retinal oil droplets in

15

329 the zebra finch (*Mundy et al., 2016*). Although several studies have investigated

330 the role of gene-environment in animal coloration, convergent phenotypes

331 commonly arise from a single pigment-mediated independent change. Our

332 study reveals a different mechanism in which βCBP, as a red signaling, has an

333 integrative and palette effect on black and green body color change depending

334 on the population density in locusts .

335 In our study, single βCBP or β-carotene cannot produce pigment

336 deposition in the black tergum integuments of locusts. βCBP only combine β-

337 carotene to form red pigment complex for producing the black pattern of

338 gregarious locusts. Previous studies in other species have similarly reported

339 that pigment-binding protein can uptake and bind pigment to affect coloration

340 (*Sakudoh et al., 2011; Sakudoh et al., 2007; W. Wang et al., 2014*). In the

341 silkworm *Bombyx mori*, the yellow cocoon color is determined by the

342 carotenoid-binding protein gene, which controls the uptake of carotenoids in the

343 silk gland (*Sakudoh et al., 2007*). *Carotenoid-binding protein* mutation produces

344 colorless hemolymph and white cocoons, indicating that carotenoid-binding

345 protein plays a central role in cocoon color pigmentation (*Sakudoh et al., 2007;*

346 *W. Wang et al., 2014*). Mammals often obtain carotenoids by eating plants

347 (*Avalos and Limon, 2015; Bryon et al., 2017; Toews et al., 2017*). Once

348 absorbed, carotenoids are transported by lipoproteins, which are homologs of

349 CBP in insects, through the bloodstream to the target tissues. In this process,

350 the abundance and nature of lipoproteins limit the capacity to obtain

351   carotenoids (*McGraw*, *2006*). As the same, β-carotene-binding protein, as a key

352   mediator of body color production, controls β-carotene content and absorption

353   to produce red color, which is superposed on the background color of

354   gregarious locus to yield the black pattern.

355   Our results show that the black pattern of gregarious locusts is not caused

356   by an increase in melanin but is caused by the interaction of different pigments.

357   This pigment interaction has a colored palette effect that results in black

358   coloration due to the accumulation of red color β-carotene pigments in the

359   presence of blue and yellow pigments. The disappearance of the red pigment

360   in the gregarious locusts led to the emergence of green color, which is the

361   typical body color of solitary locusts. By elucidating the mechanism by which

362   different types of pigments interact to create transitions among color

363   polymorphisms, this study provides new information that could be useful for

364   analyzing color transitions in other organisms. In *Heliconius erato* and *Agraulis*

365   *vanillae*, optix is required for the red color pattern and coordinates between the

366   ommochrome (orange and red) and melanin (black and gray) pigment types

367   (*Zhang et al.*, *2017*). Parrots acquire their colors through regulatory changes

368   that drive the high expression of MuPKS in feather epithelia, which appear

369   green when the blue and yellow pigments are present (*Cooke et al.*, *2017*). The

370   green color of the integument of solitary locusts is obtained from a mixture of

371   blue biliverdin pigment and yellow carotenoids (*Goodwin*, *1952; Goodwin and*

372   *Srisukh*, *1951*). As expected, the expression levels of *biliverdin-binding protein*

373 and *carotenoid-binding protein* in the pronotum integument were not

374 significantly different between the gregarious and solitary locusts (*Figure 6—*

375 *figure supplement 1*), suggesting that the contents of blue biliverdin and yellow

376 carotenoid are the same in gregarious and solitary locusts. Thus, our results

377 suggest a colored palette mechanism of body color change, with the change

378 from typical gregarious-phased coloration (black) to solitary-phased coloration

379 (green) is dependent on the extent of red β-carotene bound to βCBP.

380   The color polymorphism of gregarious and solitary locusts reflects an

381 adaptive strategy to respond to changes in population density and the natural

382 environment (*Simoes et al.*, *2016*), which is consistent with the strategies of

383 other animals when encountering different selection pressures (*Cuthill et al.*,

384 *2017*). The contrasting body coloration of gregarious locusts may allow mutual

385 recognition and warning against predators in swarms. In addition, crowding

386 stimuli, including the stress of a high population density and emission of an

387 aggregative pheromone, may induce group migration (*Caro*, *2009; Sword*,

388 *2002*). By contrast, the uniform cryptic color of solitary locusts may reduce the

389 likelihood of detection and risk of predation, similar to the role of crypsis in other

390 organisms (*Caro*, *2009; Hemmi et al.*, *2006*). Animal coloration is a prominent

391 phenotypical feature that serves multiple important functions, including social

392 signaling, antipredator defense, parasitic exploitation, thermoregulation, and

393 protection from ultraviolet light, microbes, and abrasion (*Bell et al.*, *2017; Caro*

394 *et al.*, *2016; Cuthill et al.*, *2017; Duarte et al.*, *2017; Duarte et al.*, *2016*).

18

395 Therefore, the mechanisms of color variation are highly conserved and can

396 offer insights into the adaptive evolution of gene regulation. Our study shows a

397 new "palette effect" mechanism by which the red βCBP–β-carotene pigment

398 complex can act as a switch to coordinate between black and green coloration.

399 This mechanism of color pattern change may be evolutionarily conserved

400 among multiple species, although additional functional work is needed to

401 assess this hypothesis.

402 **Materials and Methods**

403 **Insects**

404 All insects used in the experiments were reared in the same locust colonies at

405 the Institute of Zoology, Chinese Academy of Sciences, Beijing, China.

406 Gregarious nymphs were reared in large, well-ventilated cages (400 insects per

407 case). Solitary nymphs were cultured alone in white metal boxes supplied with

408 charcoal-filtered compressed air. Both colonies were reared under a 14:10 light:

409 dark photo regime at 30 ± 2 °C (*Kang et al., 2004*).

410 **Strand-specific RNA sequencing of the integument**

411 The pronotum integument was dissected from gregarious or solitary fourth-

412 instar nymphs. Total RNA of the pronotum samples was extracted using TRIzol

413 (Invitrogen) and treated with DNase I following the manufacturer's instructions.

414 RNA quality was assessed using an Agilent 2100 Bioanalyzer (Agilent) to verify

415 RNA integrity. cDNA libraries were prepared according to Illumina's protocols.

416 The adaptor sequences in the raw sequencing data were filtered using

417 Trimmomatic-0.30 (*Bolger et al., 2014*). We performed the de novo

418 transcriptome assembly by using Trinity software (trinityrnaseq r20140717).

419 Clean reads were mapped to the de novo transcriptome assembly in the

420 accompanying script in Trinity software. The number of total reads was

421 normalized using fragments per kilobase of transcripts per million reads

422 mapped. The significance of differences between the test and control groups

423 was based on *p* values with false discovery rate correction. DEGs with

424 significance at corrected $p < 0.05$ in each comparison were determined using

425 the run_DE_analysis in the R environment. The RNA-seq data were deposited

426 in the Sequence Read Archive Database of NCBI (accession no.

427 PRJNA399053).

428 **Assays of quantitative PCR for genes**

429 Total RNA was isolated from the integument by using TRIzol (Invitrogen). The

430 Moloney murine leukemia virus reverse transcriptase (Promega, USA) was

431 used to prepare the oligo (dT)-primed cDNA. mRNAs were subjected to qPCR

432 by using SYBR Green gene expression assays in accordance with the

433 manufacturer's instructions (Tiangen). qPCR was performed on a LightCycler®

434 480 instrument (Roche). *β-actin* was used as the internal control. Dissociation

435 curves were determined for each mRNA to confirm unique amplification. The

436 qPCR primers used are listed in *Supplementary files 1*. All of the qRT–PCR

437 reactions were performed in six biological replicates. Four integument samples

438 were used in each biological replicate.

βCBP immunohistochemical assay

βCBP was detected in the integument via immunohistochemistry. The integument was fixed in 4% paraformaldehyde overnight. Paraffin-embedded integument tissue slides (5 μm thick) were deparaffinized in xylene and rehydrated with an ethanol gradient. The samples were blocked with 5% BSA for 30 min and then incubated with an anti-βCBP antiserum (1 : 200) for 2 h. The slides were washed and incubated for 1 h with Alexa Fluor-488 goat anti-rabbit secondary antibody (Life Technologies). Hoechst (1 : 500) was used for nuclei staining. The βCBP signals were detected using an LSM 710 confocal fluorescence microscope (Zeiss).

Transcript knockdown via RNAi

To knockdown the transcript of *βCBP*, dsRNA was synthesized using the T7 RiboMAXTM Express RNAi System (Promega, USA) following the manufacturer's instructions. Each insect was injected with 3 μg of dsRNA three times at day 3 for the second-instar nymphs and at days 1 and 5 for the third-instar nymphs. Control nymphs were injected with an equivalent amount of *dsGFP*–RNA. Nymphs that showed body color changes were used for the extraction. Six abnormal nymphs and six control nymphs were used for CBP immunohistochemistry.

Feeding β-carotene assay

Solitary nymphs of 3-day-old second instars were fed with a synthetic diet containing β-carotene and subjected to crowding for two stadiums before

21

461 calculating the body color phenotype statistics. The composition of the basic

462 synthetic diet used in the experiment is shown in *Supplementary files 2*. Control

463 insects were fed a synthetic diet without β-carotene and exposed to crowding.

464 Rearing jars were cleaned and fresh diets were provided every day. A total of

465 29 nymphs were fed a synthetic diet in each of the treatment and control groups.

466 **Body color rescue experiment in vivo**

467 A rescue experiment was performed with solitary locusts. Approximately 30

468 second-instar nymphs were fed a synthetic diet containing β-carotene and then

469 subjected to crowding. One stadium later, these nymphs were injected with 3

470 μg *dsβCBP* or *dsGFP* control and then isolated. One stadium after the dsRNA

471 injection, the nymphs were subjected to body color analysis.

472 **Immunoelectron microscopy**

473 For βCBP immunolabeling, integuments were fixed with 2.5% glutaraldehyde

474 in 0.1 M phosphate buffer. After dehydration in a graded alcohol series,

475 specimens were embedded in LR White resin and polymerized at 60 °C.

476 Ultrathin sections were blocked with phosphate-buffered saline (PBS)

477 containing 1% BSA, 0.2% Tween-20, and 0.2% gelatin before labeling with the

478 CBP polyclonal antibody (1 : 1000). A gold-conjugated (10 nm) secondary

479 rabbit antibody was used to visualize the binding sites through TEM (Ruli H-

480 750, Japan).

481 **β-carotene binding assay in vitro and in vivo**

482 A β-carotene-binding experiment in vitro was conducted as previously

22

483   described (*Tabunoki et al., 2002*). Purified rβCBP was resuspended in PBS

484   binding buffer containing 1 mg/mL BSA. Samples containing 50 M rCBP and

485   100 M β-carotene were incubated in 1 mL of binding buffer for 3 h at 25 °C. The

486   control experiments were performed using the same procedure without the use

487   of purified rβCBP or BSA. Anti-CBP rabbit IgG–protein A-Sepharose was added

488   to the reaction mixture and incubated for 4 h at 4 °C. The protein A-Sepharose–

489   rβCBP–β-carotene complex was collected by centrifugation at 13, 000 g for 10

490   s. To remove the unbound β-carotene, the pellets were washed 5 times with 20

491   mM Tris-HCl (pH 7.6) containing 150 mM NaCl, 1% Nonidet P-40, protease

492   inhibitor mixture, and 1 mg/mL BSA. Binding of β-carotene to rβCBP was

493   confirmed by the presence of red-colored precipitate.

494   For the β-carotene binding experiment in vivo, approximately 200 pronotum

495   integuments from gregarious individuals were collected and homogenized in

496   ice-cold PBS buffer containing protease inhibitor. βCBP antibody or rabbit IgG,

497   which was used as a negative control, and protein A-Sepharose was added to

498   the homogenate and incubated at 4 °C overnight. The protein A-Sepharose-

499   βCBP–β-carotene complex was collected by centrifugation at 13, 000 g for 30

500   s. The pellets were washed five times to remove the unbound β-carotene.

501   **β-carotene quantification of the pronotum tissue extracts**

502   The β-carotene content of locust pronotum integument was quantified using

503   reverse-phase HPLC and DAD. Pronotum tissues of locust nymphs were

504   rapidly dissected and stored in liquid nitrogen. Thirty pronotums were

23

505 homogenized and lysed in lysate buffer. After incubation with βCBP antibody–

506 protein A-sepharose at 4 °C overnight, the specimens were placed in a 50 mL

507 centrifuge tube containing a mixture of n-hexane, ethanol, and acetone (2 : 1 :

508 1, v : v : v). The tissue samples were sonicated at 5–10 °C for 15 min and then

509 centrifuged at 6, 800 g for 10 min. The upper layer extract and the ether extract

510 of the lower layer residual solution were collected in another centrifuge tube.

511 The same sample was re-extracted twice according to the same protocol as

512 described above. Then, 2 mL of ether and 2 mL of distilled water were added

513 to the lower layer collection tube and sonicated at 4 °C for 5 min. Following, the

514 upper phase was collected. All of the extracts were combined and dried using

515 a lyophilizer. The dried residue was dissolved in 2 mL of methyl tertbutyl ether

516 (MTBE) and 2 mL of a KOH: methanol mixture (1 : 9, w : v). After over 10 h in

517 darkness, 2 mL of MTBE and 2 mL of distilled water were added to the mixture.

518 Then, the upper extract was collected and dried. This dried residue was

519 dissolved in 200 μL of MTBE containing 0.1% BHT and filtered through 0.22

520 μm filters. The filtered samples were automatically loaded into the reverse

521 phase HPLC system, which contained a carotene C30 column (250 mm × 4.6

522 mm, 5 μm, YMC, Japan), at a flow rate of 1 mL/min. The gradient elution

523 method consisted of an initial 10 min of 71.2% acetonitrile, 23.8% methanol,

524 and 5.0% H2O, followed by a linear gradient of 19.5% acetonitrile, 6.5%

525 methanol, and 74.0% MTBE for 31 min. Data analysis was conducted with

526 Agilent ChemStation software. β-carotene was quantified using an external

527   standard.

Statistical analysis

SPSS 17.0 software (SPSS, Inc.) was used for statistical analysis. Differences between treatments were evaluated using either Student's *t*-test or one-way ANOVA followed by Tukey's test for multiple comparisons. A *p* value of < 0.05 was considered statistically significant. All of the results are expressed as the means ± SEM.

Author contributions

L.K., M.Y. and Y.W. designed the study; M.Y., Y.W. and Q.L. performed and analyzed the biological experiments; J.Z., Z.L., F.J., H.W. and X.G. contributed reagents/materials/analysis tools; M.Y., L.K., Y.W. and Q.L. wrote the manuscript.

Author ORCIDs

Le Kang, http://orcid.org/0000-0003-4262-2329

549   Jianzhen Zhang, https://orcid.org/0000-0003-3400-0044

550   **Declaration of Interests**

551   The authors declare no competing interests.

552   **References**

553   **Applebaum SW**, Avisar E, Heifetz Y. 1997. Juvenile hormone and locust phase.
554   *Archives of Insect Biochemistry and Physiology* **35**: 375-391. doi:Doi
555   10.1002/(Sici)1520-6327(1997)35:4<375::Aid-Arch3>3.0.Co;2-R,   PMID:
556   ISI:A1997XG47400003

557   **Avalos J**, Limon MC. 2015. Biological roles of fungal carotenoids. *Current Genetics*
558   **61**: 309-324. doi:10.1007/s00294-014-0454-x, PMID: WOS:000358180000009

559   **Bell RC**, Webster GN, Whiting MJ. 2017. Breeding biology and the evolution of
560   dynamic sexual dichromatism in frogs. *Journal of evolutionary biology* **30**:
561   2104-2115. doi:10.1111/jeb.13170, PMID: 28833835

562   **Bhosale P**, Bernstein PS. 2007. Vertebrate and invertebrate carotenoid-binding proteins.
563   *Archives of biochemistry and biophysics* **458**: 121-127.
564   doi:10.1016/j.abb.2006.10.005, PMID: 17188641

565   **Bolger AM**, Lohse M, Usadel B. 2014. Trimmomatic: a flexible trimmer for Illumina
566   sequence data. *Bioinformatics* **30**: 2114-2120.
567   doi:10.1093/bioinformatics/btu170, PMID: 24695404

568   **Bryon A**, Kurlovs AH, Dermauw W, Greenhalgh R, Riga M, Grbic M, Tirry L, Osakabe
569   M, Vontas J, Clark RM, Van Leeuwen T. 2017. Disruption of a horizontally
570   transferred phytoene desaturase abolishes carotenoid accumulation and diapause in
571   Tetranychus urticae. *Proceedings of the National Academy of Sciences of the*
572   *United States of America* **114**: E5871-E5880. doi:10.1073/pnas.1706865114,
573   PMID: 28674017

574   **Burmeister SS**, Jarvis ED, Fernald RD. 2005. Rapid behavioral and genomic responses
575   to social opportunity. *PLoS biology* **3**: e363. doi:10.1371/journal.pbio.0030363,
576   PMID: 16216088

577   **Caro T**. 2009. Contrasting coloration in terrestrial mammals. *Philosophical*
578   *transactions of the Royal Society of London. Series B, Biological sciences* **364**:
579   537-548. doi:10.1098/rstb.2008.0221, PMID: 18990666

580   **Caro T**, Sherratt TN, Stevens M. 2016. The ecology of multiple colour defences.
581   *Evolutionary Ecology* **30**: 797-809. doi:10.1007/s10682-016-9854-3, PMID:
582   WOS:000383769100001

583   **Cooke TF**, Fischer CR, Wu P, Jiang TX, Xie KT, Kuo J, Doctorov E, Zehnder A,
584   Khosla C, Chuong CM, Bustamante CD. 2017. Genetic Mapping and Biochemical
585   Basis of Yellow Feather Pigmentation in Budgerigars. *Cell* **171**: 427-439 e421.
586   doi:10.1016/j.cell.2017.08.016, PMID: 28985565

587   **Cuthill IC**, Allen WL, Arbuckle K, Caspers B, Chaplin G, Hauber ME, Hill GE,
588   Jablonski NG, Jiggins CD, Kelber A, Mappes J, Marshall J, Merrill R, Osorio D,

Prum R, Roberts NW, Roulin A, Rowland HM, Sherratt TN, Skelhorn J, Speed MP, Stevens M, Stoddard MC, Stuart-Fox D, Talas L, Tibbetts E, Caro T. 2017. The biology of color. *Science* **357**: 470-477. doi:10.1126/science.aan0221, PMID: 28774901

D'Orazio JA, Nobuhisa T, Cui R, Arya M, Spry M, Wakamatsu K, Igras V, Kunisada T, Granter SR, Nishimura EK, Ito S, Fisher DE. 2006. Topical drug rescue strategy and skin protection based on the role of Mc1r in UV-induced tanning. *Nature* **443**: 340-344. doi:10.1038/nature05098, PMID: 16988713

Duarte RC, Flores AAV, Stevens M. 2017. Camouflage through colour change: mechanisms, adaptive value and ecological significance. *Philosophical transactions of the Royal Society of London. Series B, Biological sciences* **372**. doi:10.1098/rstb.2016.0342, PMID: 28533459

Duarte RC, Stevens M, Flores AA. 2016. Shape, colour plasticity, and habitat use indicate morph-specific camouflage strategies in a marine shrimp. *Bmc Evolutionary Biology* **16**: 218. doi:10.1186/s12862-016-0796-8, PMID: 27756220

Futahashi R, Fujiwara H. 2008. Juvenile hormone regulates butterfly larval pattern switches. *Science* **319**: 1061. doi:10.1126/science.1149786, PMID: 18292334

Futahashi R, Kurita R, Mano H, Fukatsu T. 2012. Redox alters yellow dragonflies into red. *Proceedings of the National Academy of Sciences of the United States of America* **109**: 12626-12631. doi:10.1073/pnas.1207114109, PMID: 22778425

Goodwin TW. 1952. The Biochemistry of Locust Pigmentation. *Biological Reviews* **27**: 439-460. doi:10.1111/j.1469-185X.1952.tb01514.x, PMID: ISI:A1952UX07900004

Goodwin TW, Srisukh S. 1951. Biochemistry of Locusts; The Green Pigment of the Haemolymph and Integument of Solitary Locusts (Locusta-Migratoria-Migratorioides, R and F, and Schistocerca-Gregaria, Forsk). *Biochemical Journal* **48**: 199-203. PMID: 14820828

Guo W, Wang XH, Ma ZY, Xue LA, Han JY, Yu D, Kang L. 2011. CSP and Takeout Genes Modulate the Switch between Attraction and Repulsion during Behavioral Phase Change in the Migratory Locust. *Plos Genetics* **7**. doi:10.1371/journal.pgen.1001291, PMID: 21304893

Hemmi JM, Marshall J, Pix W, Vorobyev M, Zeil J. 2006. The variable colours of the fiddler crab Uca vomeris and their relation to background and predation. *Journal of Experimental Biology* **209**: 4140-4153. doi:10.1242/jeb.02483, PMID: 17023607

Henderson AJ, Lasselin J, Lekander M, Olsson MJ, Powis SJ, Axelsson J, Perrett DI. 2016. Skin colour changes during experimentally-induced sickness. *Brain Behav Immun*. doi:10.1016/j.bbi.2016.11.008, PMID: 27847284

Hubbard JK, Uy JA, Hauber ME, Hoekstra HE, Safran RJ. 2010. Vertebrate pigmentation: from underlying genes to adaptive function. *Trends in Genetics* **26**: 231-239. doi:10.1016/j.tig.2010.02.002, PMID: 20381892

Kang L, Chen X, Zhou Y, Liu B, Zheng W, Li R, Wang J, Yu J. 2004. The analysis of large-scale gene expression correlated to the phase changes of the migratory locust. *Proceedings of the National Academy of Sciences of the United States of America*

633   **101**: 17611-17615. doi:10.1073/pnas.0407753101, PMID: 15591108

634   **Ma ZY**, Guo W, Guo XJ, Wang X, Kang L. 2011. Modulation of behavioral phase
635   changes of the migratory locust by the catecholamine metabolic pathway.
636   *Proceedings of the National Academy of Sciences of the United States of America*
637   **108**: 3882-3887. doi:10.1073/pnas.1015098108, PMID: 21325054

638   **Mathger LM**. 2003. Rapid colour changes in multilayer reflecting stripes in the
639   paradise whiptail, Pentapodus paradiseus. *Journal of Experimental Biology* **206**:
640   3607-3613. doi:10.1242/jeb.00599, PMID: 12966052

641   **McGraw KJ**. 2006. Sex steroid dependence of carotenoid-based coloration in female
642   zebra finches. *Physiology & Behavior* **88**: 347-352.
643   doi:10.1016/j.physbeh.2006.04.003, PMID: 16740280

644   **Moran NA**, Jarvik T. 2010. Lateral transfer of genes from fungi underlies carotenoid
645   production in aphids. *Science* **328**: 624-627. doi:10.1126/science.1187113,
646   PMID: 20431015

647   **Mundy NI**, Stapley J, Bennison C, Tucker R, Twyman H, Kim KW, Burke T, Birkhead
648   TR, Andersson S, Slate J. 2016. Red Carotenoid Coloration in the Zebra Finch Is
649   Controlled by a Cytochrome P450 Gene Cluster. *Current Biology* **26**: 1435-1440.
650   doi:10.1016/j.cub.2016.04.047, PMID: 27212402

651   **Pener MP**. 1991. Locust Phase Polymorphism and its Endocrine Relations. *Advances*
652   *in Insect Physiology* **23**: 1-79. doi:10.1016/s0065-2806(08)60091-0, PMID:
653   ISI:A1991MC40700001

654   **Pener MP**, Simpson SJ. 2009. Locust Phase Polyphenism: An Update. *Advances in*
655   *Insect Physiology* **36**: 1-272. doi:10.1016/S0065-2806(08)36001-9, PMID:
656   WOS:000273300400001

657   **Sakudoh T**, Nakashima T, Kuroki Y, Fujiyama A, Kohara Y, Honda N, Fujimoto H,
658   Shimada T, Nakagaki M, Banno Y, Tsuchida K. 2011. Diversity in copy number and
659   structure of a silkworm morphogenetic gene as a result of domestication. *Genetics*
660   **187**: 965-976. doi:10.1534/genetics.110.124982, PMID: 21242537

661   **Sakudoh T**, Sezutsu H, Nakashima T, Kobayashi I, Fujimoto H, Uchino K, Banno Y,
662   Iwano H, Maekawa H, Tamura T, Kataoka H, Tsuchida K. 2007. Carotenoid silk
663   coloration is controlled by a carotenoid-binding protein, a product of the Yellow
664   blood gene. *Proceedings of the National Academy of Sciences of the United States*
665   *of America* **104**: 8941-8946. doi:10.1073/pnas.0702860104, PMID: 17496138

666   **Simoes PM**, Ott SR, Niven JE. 2016. Environmental Adaptation, Phenotypic Plasticity,
667   and Associative Learning in Insects: The Desert Locust as a Case Study.
668   *Integrative and Comparative Biology* **56**: 914-924. doi:10.1093/icb/icw100,
669   PMID: 27549202

670   **Stuart-Fox D**, Moussalli A. 2008. Selection for social signalling drives the evolution
671   of chameleon colour change. *PLoS biology* **6**: e25.
672   doi:10.1371/journal.pbio.0060025, PMID: 18232740

673   **Sword GA**. 2002. A role for phenotypic plasticity in the evolution of aposematism.
674   *Proceedings. Biological sciences* **269**: 1639-1644. doi:10.1098/rspb.2002.2060,
675   PMID: 12204123

676   **Tabadkani SM**, Ahsaei SM, Hosseininaveh V, Nozari J. 2013. Food stress prompts

677   dispersal behavior in apterous pea aphids: do activated aphids incur energy loss?
678   *Physiology & Behavior* **110**: 221-225. doi:10.1016/j.physbeh.2012.12.004, PMID:
679   23262143

680 **Tabunoki H**, Sugiyama H, Tanaka Y, Fujii H, Banno Y, Jouni ZE, Kobayashi M, Sato
681   R, Maekawa H, Tsuchida K. 2002. Isolation, characterization, and cDNA sequence
682   of a carotenoid binding protein from the silk gland of Bombyx mori larvae. *The*
683   *Journal of biological chemistry* **277**: 32133-32140. doi:10.1074/jbc.M204507200,
684   PMID: 12052833

685 **Tanaka S**. 1993. Hormonal Deficiency Causing Albinism in Locusta-Migratoria.
686   *Zoological Science* **10**: 467-471. PMID: ISI:A1993LN37500010

687 **Tanaka S**. 2000. The role of [His(7)]-corazonin in the control of body-color
688   polymorphism in the migratory locust, Locusta migratoria (Orthoptera : Acrididae).
689   *Journal of Insect Physiology* **46**: 1169-1176. doi:Doi 10.1016/S0022-
690   1910(99)00228-0, PMID: 10818224

691 **Teyssier J**, Saenko SV, van der Marel D, Milinkovitch MC. 2015. Photonic crystals
692   cause active colour change in chameleons. *Nature communications* **6**: 6368.
693   doi:10.1038/ncomms7368, PMID: 25757068

694 **Toews DPL**, Hofmeister NR, Taylor SA. 2017. The Evolution and Genetics of
695   Carotenoid Processing in Animals. *Trends in Genetics* **33**: 171-182.
696   doi:10.1016/j.tig.2017.01.002, PMID: 28174022

697 **Valverde JP**, Schielzeth H. 2015. What triggers colour change? Effects of background
698   colour and temperature on the development of an alpine grasshopper. *Bmc*
699   *Evolutionary Biology* **15**. doi:10.1186/s12862-015-0419-9, PMID: 26293296

700 **Wang W**, Huang MH, Dong XL, Chai CL, Pan CX, Tang H, Chen YH, Dai FY, Pan
701   MH, Lu C. 2014. Combined effect of Cameo2 and CBP on the cellular uptake of
702   lutein in the silkworm, Bombyx mori. *Plos One* **9**: e86594.
703   doi:10.1371/journal.pone.0086594, PMID: 24475153

704 **Wang X**, Fang X, Yang P, Jiang X, Jiang F, Zhao D, Li B, Cui F, Wei J, Ma C, Wang Y,
705   He J, Luo Y, Wang Z, Guo X, Guo W, Wang X, Zhang Y, Yang M, Hao S, Chen B,
706   Ma Z, Yu D, Xiong Z, Zhu Y, Fan D, Han L, Wang B, Chen Y, Wang J, Yang L, Zhao
707   W, Feng Y, Chen G, Lian J, Li Q, Huang Z, Yao X, Lv N, Zhang G, Li Y, Wang J,
708   Wang J, Zhu B, Kang L. 2014. The locust genome provides insight into swarm
709   formation and long-distance flight. *Nature communications* **5**: 1-9.
710   doi:10.1038/ncomms3957, PMID: 24423660

711 **Wang XH**, Kang L. 2014. Molecular mechanisms of phase change in locusts. *Annual*
712   *Review of Entomology* **59**: 225-244. doi:10.1146/annurev-ento-011613-162019,
713   PMID: 24160426

714 **Wu R**, Wu Z, Wang X, Yang P, Yu D, Zhao C, Xu G, Kang L. 2012a. Metabolomic
715   analysis reveals that carnitines are key regulatory metabolites in phase transition of
716   the locusts. *Proceedings of the National Academy of Sciences of the United States*
717   *of America* **109**: 3259-3263. doi:10.1073/pnas.1119155109, PMID: 22328148

718 **Wu R**, Wu Z, Wang X, Yang P, Yu D, Zhao C, Xu G, Kang L. 2012b. Metabolomic
719   analysis reveals that carnitines are key regulatory metabolites in phase transition of
720   the locusts. *Proceedings of the National Academy of Sciences* **109**: 3259-3263.

721   doi:10.1073/pnas.1119155109, PMID: 22328148

722 **Xiong G**, Tong X, Gai T, Li C, Qiao L, Monteiro A, Hu H, Han M, Ding X, Wu S,
723   Xiang Z, Lu C, Dai F. 2017. Body Shape and Coloration of Silkworm Larvae Are
724   Influenced by a Novel Cuticular Protein. *Genetics* **207**: 1053-1066.
725   doi:10.1534/genetics.117.300300, PMID: 28923848

726 **Yang ML**, Wei YY, Jiang F, Wang YL, Guo XJ, He J, Kang L. 2014. MicroRNA-133
727   inhibits behavioral aggregation by controlling dopamine synthesis in locusts. *Plos*
728   *Genetics* **10**: e1004206. doi:10.1371/journal.pgen.1004206, PMID: 24586212

729 **Zhang L**, Mazo-Vargas A, Reed RD. 2017. Single master regulatory gene coordinates
730   the evolution and development of butterfly color and iridescence. *Proceedings of*
731   *the National Academy of Sciences of the United States of America* **114**: 10707-
732   10712. doi:10.1073/pnas.1709058114, PMID: 28923944

733

734

735

736

737
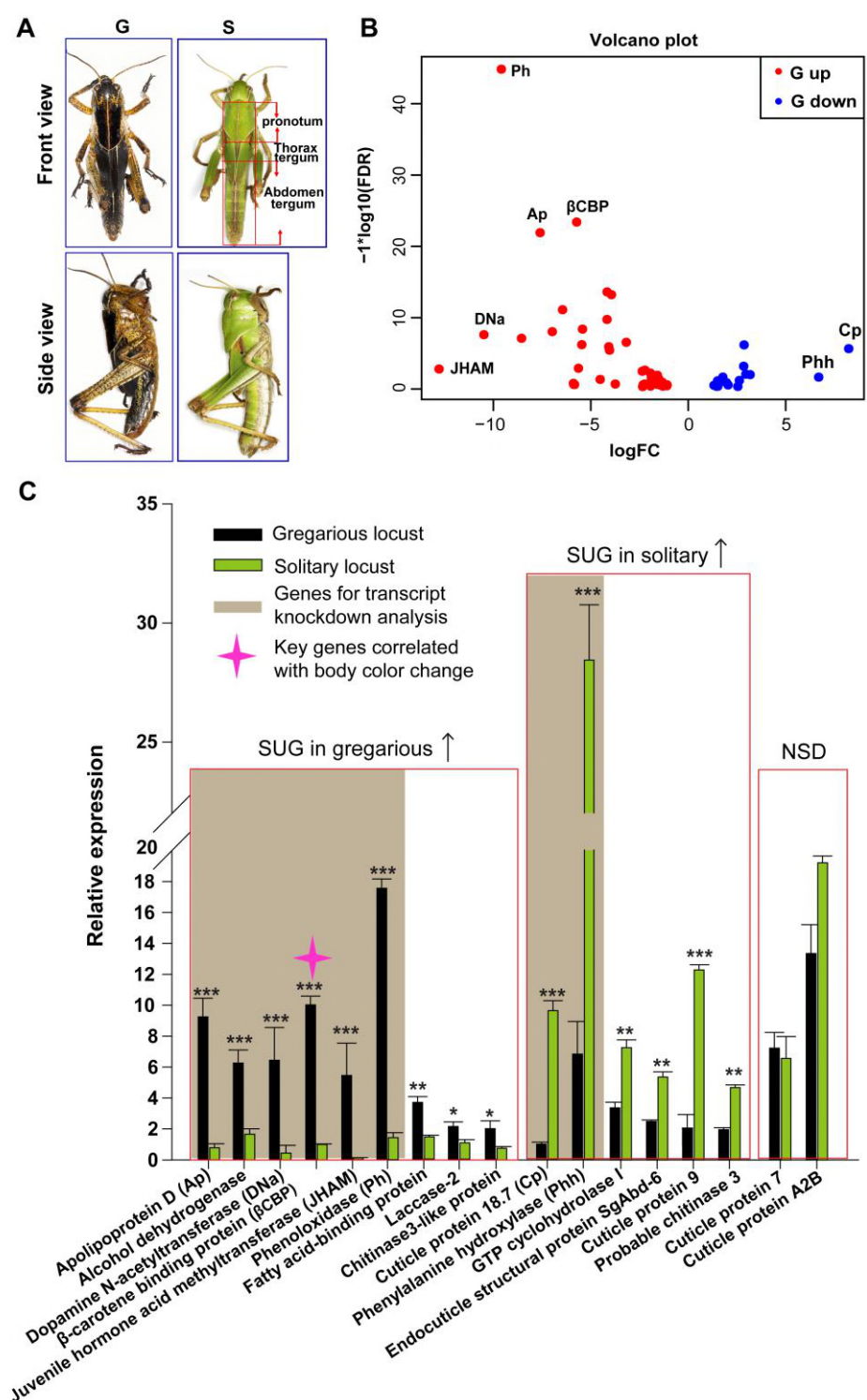
738

739

740

741

742

743

744

745

746

747

748

Figure 1. Identification of β-carotene-binding protein (βCBP) as a target associated with body color changes between gregarious and solitary locusts.

(A) Body colors of typical gregarious and solitary nymphs. The tergums include

771   pronotum, thorax tergum and abdomen tergum. (B) Logarithmic fold alterations

772   of 68 differentially expressed genes (DEGs) associated with animal coloration

773   between gregarious and solitary locusts are shown in the volcano plot diagram

774   generated from genome-wide RNA-Seq. Red and blue dots indicate up- and

775   down regulated genes, respectively, in the gregarious locusts (n = 3 samples,

776   10 integuments/sample). (C) The top 17 DEGs (Log FC > 2.8, FDR < 1e−5)

777   among the 68 genes from the volcano plot diagram were confirmed in the

778   gregarious and solitary integuments via qPCR (n = 6 samples; 8

779   integuments/sample; Student's *t*-test; red boxes indicate significantly up

780   regulated genes (SUG) in gregarious/solitary locusts and no significant

781   difference between gregarious and solitary locusts; *$p < 0.05$; **$p < 0.01$;

782   ***$p < 0.001$). Brown shades denote the eight genes used for transcript

783   knockdown analysis. The red star in the histogram indicate the identified target

784   gene that correlates with body color change in the phase transition of locusts.

785   The following figure supplement is available for figure 1:

786   **Source data 1.** Numerical data that are represented as graphs in *Figure 1C*.

787   **Figure supplement 1. Transcriptomic profiles of locust pronotum**

788   **integuments revealed by strand-specific RNA-seq.**

789   **Figure supplement 2. βCBP fosters the body color change from the**

790   **gregarious pattern to the solitary pattern.**
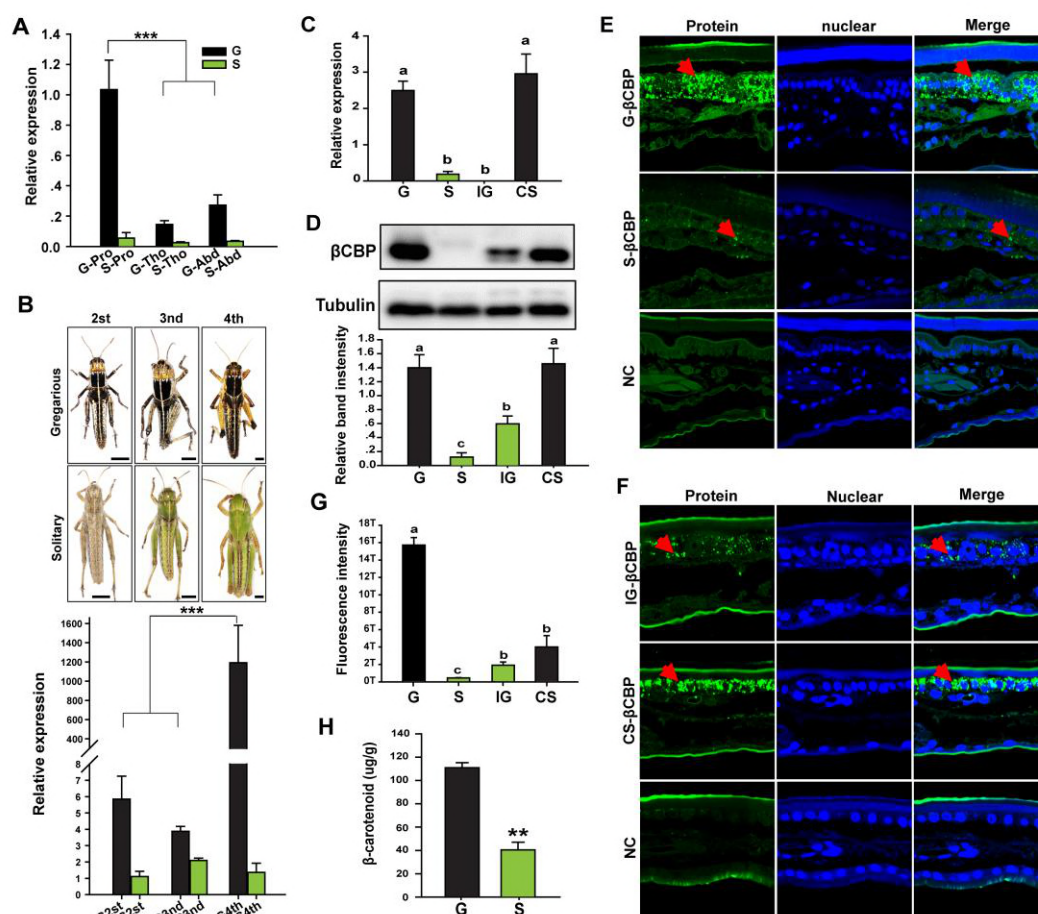
791

792

793

794

Figure 2. Expression or distribution of βCBP and its binding β-carotene shows phase-specific patterns. (A) *βCBP* expression in the tergums of different body segments of locusts in the gregarious (G) and solitary (S) phases. Pro: Pronotum; Tho: Thorax; Abd: Abdomen. (B) *βCBP* expression in the pronotums of different instars of gregarious (G) and solitary (S) nymphs. Body color phenotypes of typical gregarious and solitary nymphs in the second (2st), third (3nd), and fourth (4th) instar are shown. The scale is 2 mm for each nymph. mRNA expression of *βCBP* was quantified by using qRT–PCR. qPCR data are shown as the means ± SEM (n = 6). *$p < 0.05$; **$p < 0.01$; ***$p < 0.001$. (C, D)

33

804   mRNA (C) and protein (D) expression levels of βCBP were determined in the

805   integuments of fourth-instar gregarious (G) nymphs, solitary (S) nymphs,

806   gregarious nymphs after isolation (IG), and solitary nymphs after crowding (CS)

807   using qPCR and Western blot analyses. (E) Distribution analysis of CBP was

808   conducted to determine the localization and differences in abundance of CBP

809   in the integuments between the gregarious (G) and solitary (S) locusts via

810   immunohistochemistry. The red arrows indicate the areas where βCBP was

811   localized in the locust integuments. NC, negative control. Images were

812   visualized using an LSM 710 confocal fluorescence microscope (Zeiss) at a

813   magnification of 40×. (F) Expression signals for βCBP were analyzed in the

814   integuments of gregarious nymphs after isolation (IG) and solitary nymphs after

815   crowding (CS). (G) Fluorescence intensity was quantified using ZEN 2.1

816   software and expressed as the means ± SEM (n = 3). (H) β-carotene content

817   in the gregarious and solitary locust integuments was evaluated using HPLC.

818   qPCR and HPLC data are shown as the mean ± SEM (n = 6). Western blot

819   bands were quantified using densitometry, and the values are expressed as the

820   mean ± SEM (n = 3); the same letter indicates that the data are not significantly

821   different.

822   The following figure supplement is available for figure 2:

823   **Source data 1.** Numerical data that are represented as graphs in *Figure 2A,*

824   *B, C, D, G, H.*

825   **Figure supplement 1. *βCBP* expression in the different tissues of**

826   **gregarious locusts as determined by qRT–PCR.**

827   **Figure supplement 2. *βCBP* expression in the time course of gregarious**

828   **locusts.**

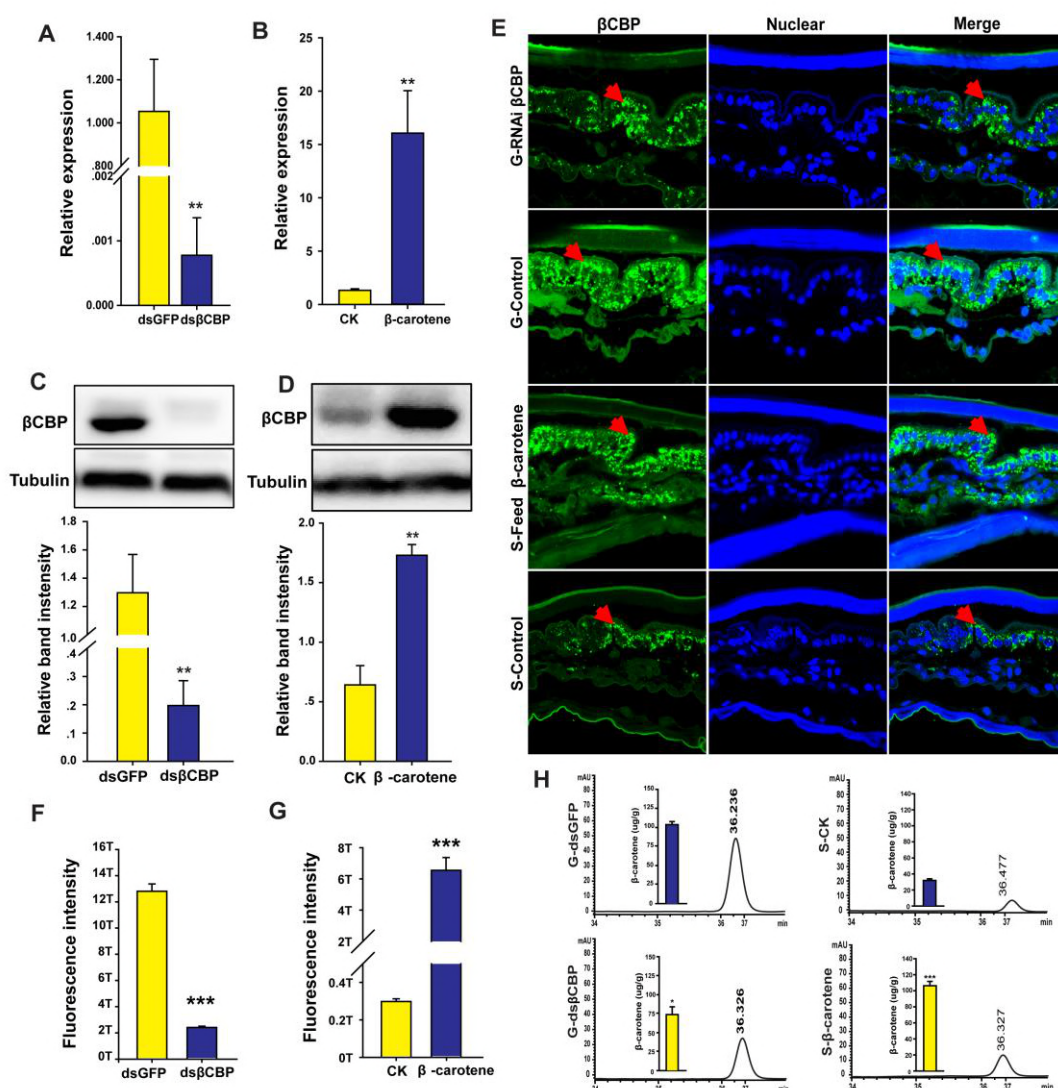829   **Figure supplement 3. *βCBP* expression in the tergum of the thorax and**

830   **abdomen of locusts.**

831

832

833

834

835

836

837

838

839

840

841

842

843

844

845

846

847

848

Figure 3. βCBP accumulates β-carotene pigment to affect pigmentation in the phase transition of locusts. (A, C) mRNA and protein expression of βCBP in the pronotum integument was quantified using qRT–PCR (A) and Western blot analyses (C) two stadiums after βCBP silencing and isolating in gregarious locusts. (B, D) mRNA and protein expression levels of βCBP in the pronotum integument were determined two stadiums after feeding with β-carotene and crowding in solitary locusts using qPCR (B) and Western blot analyses (D). (E) Fluorescence signals of βCBP were determined in gregarious (G) locusts after

857 βCBP silencing coupled with isolation and in solitary (S) locusts after feeding

858 with β-carotene diet coupled with crowding. (F, G) Fluorescence signal intensity

859 of βCBP was quantified using ZEN 2.1 software and expressed as the means

860 ± SEM (n = 3). (H) β-carotene content was evaluated in gregarious locusts after

861 βCBP silencing coupled with isolation and in solitary locusts after feeding with

862 β-carotene diet coupled with crowding by using HPLC. qPCR and HPLC data

863 are shown as the means ± SEM (n = 6). Western blot bands were quantified

864 using densitometry, and the values are expressed as the means ± SEM (n = 3);

865 *p < 0.05; **p < 0.01; ***p < 0.001.

866 The following figure supplement is available for figure 3:

867 **Source data 1.** Numerical data that are represented as graphs in *Figure 3A,*

868 *B, C, D, F, G, H.*

869 **Figure supplement 1. *βCBP* expression in the tergum of the thorax and**

870 **abdomen of locusts after RNAi *βCBP*.**

871 **Figure supplement 2. βCBP expression in the tergum of the thorax and**

872 **abdomen of solitary locusts.**

873 **Figure supplement 3. *βCBP* expression in the pronotum of solitary**

874 **locusts only pre-fed with β-carotene but no crowding by qRT–PCR.**

875

876

877

878

879

880
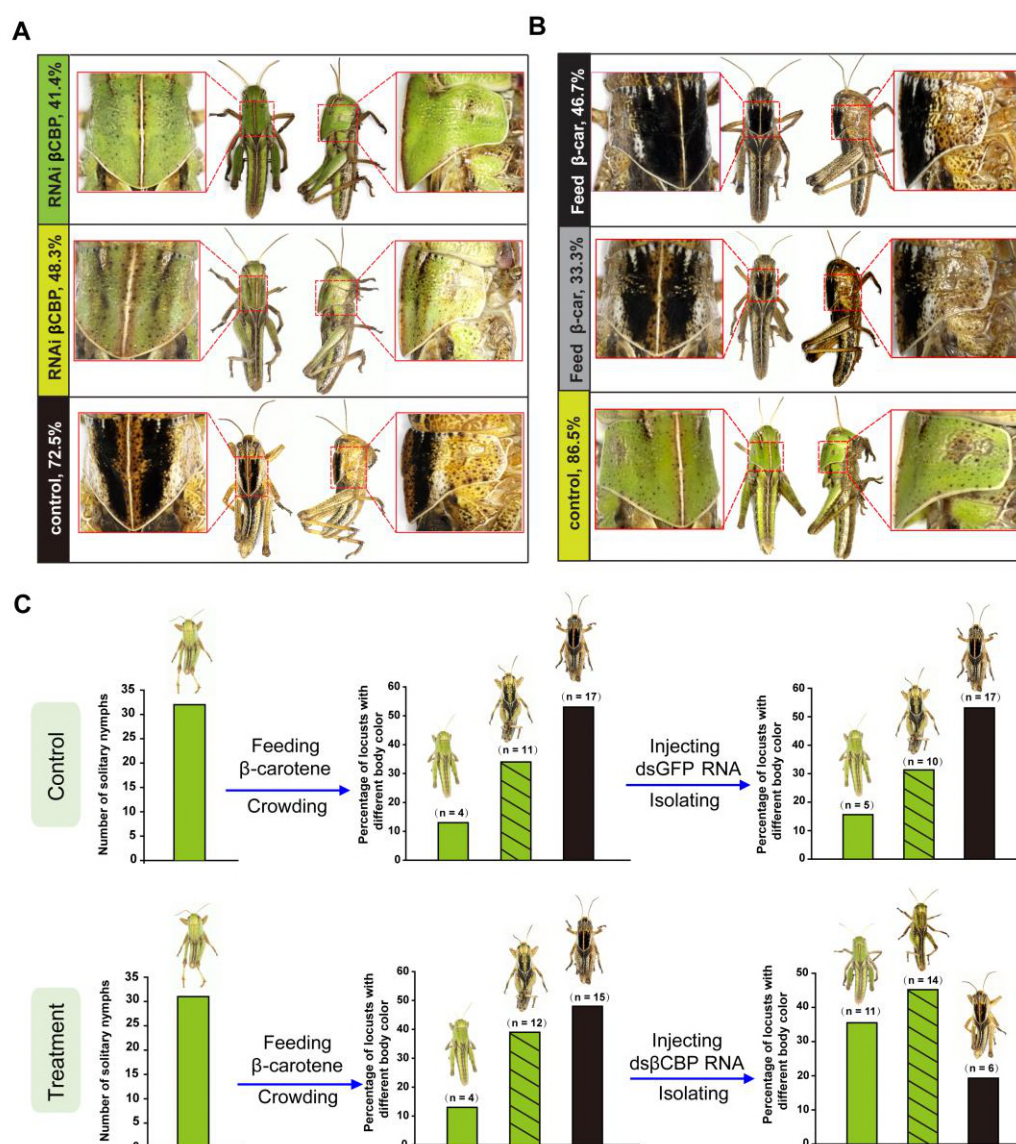
Figure 4. βCBP and its binding of β-carotene fosters the body color phase transition of the locust. (A) Effects of *βCBP* dsRNA treatment on the bod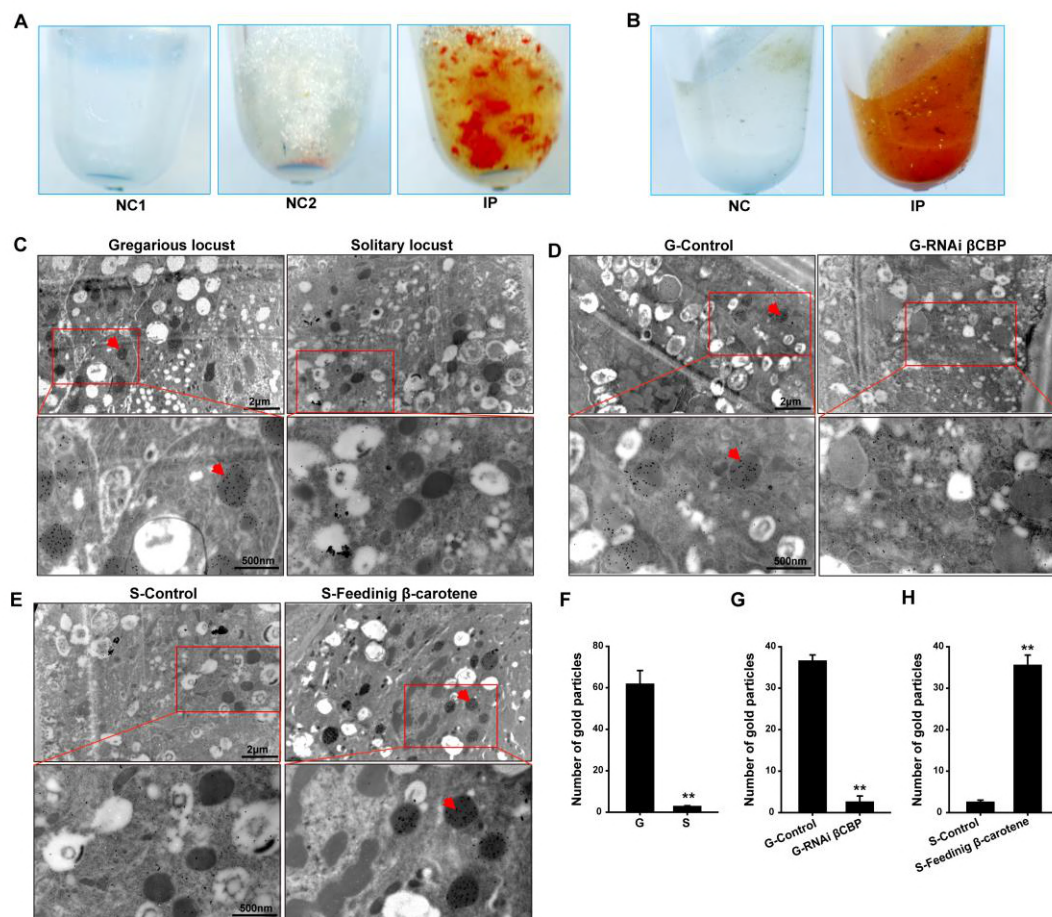y color of gregarious locusts. Each second-instar nymph was injected with 3 μg of dsRNA thrice and exposed to isolation. Control nymphs were injected with equivalent volumes of dsGFP and then isolated. (B) Effects of β-carotene feeding on the body color of solitary locusts. Solitary nymphs were fed a

38

887   synthetic diet containing β-carotene and were then subjected to crowding.

888   Control insects were fed a regular diet without β-carotene and were then

889   subjected to crowding. (C) A body color rescue experiment in solitary locusts

890   was performed by injecting dsRNA against *βCBP* at day 3 in third-instar nymphs

891   (N3D3) that had been pretreated with β-carotene feeding at day 1 as second-

892   instar nymphs (N2D1). The control group was injected with dsGFP as third-

893   instar nymphs that had been pretreated with β-carotene feeding as second-

894   instar nymphs.

895

896

897

898

899

900

901

902

903

904

905

906

907

908

Figure 5. The red complex of βCBP located in the pigment granules of integument and βCBP binding of β-carotene directly contributes to the black back pattern of gregarious locusts. (A) Red βCBP–pigment complex was confirmed by recombinant βCBP (rβCBP) incubation with β-carotene under immunoprecipitation using βCBP antibody conjugated to protein A-Sepharose. NC1, containing β-carotene without rβCBP; NC2, containing BSA and β-carotene; IP, containing β-carotene and rβCBP. (B) Red pigment accumulates in the precipitate of the locust pronotum when treated with anti-βCBP-immunoprecipitation compared with IgG-immunoprecipitation. NC, containing pronotums and IgG; IP, containing pronotums and βCBP antibody. (C) The

919   subcellular distribution of βCBP was investigated in the integuments of

920   gregarious and solitary locusts by immunoelectron microscopy. (D, E)

921   Immunogold labeling signals of βCBP were comparatively analyzed in the

922   integuments of gregarious locusts after injection with *βCBP* dsRNAs and

923   subsequent isolation and (D) in the integuments of solitary integuments after

924   feeding with β-carotene diet followed by crowding (E). (F, G, H) Average

925   number of gold particles in three randomly selected pigment granules in

926   sections from various treatments. Variation is calculated based on three

927   biological replicates (n = 3, **p < 0.01). All sections were probed with anti-βCBP,

928   followed by protein A-gold conjugate. Images outlined with red squares are

929   magnified at 30,000 × using the Ruli H-750 TEM (Japan). The red arrow

930   indicates the gold particles of βCBP located in the pigment granules.

931   The following figure supplement is available for figure 5:

932   **Source data 1.** Numerical data that are represented as graphs in *Figure 5F,*

933   *G, H.*

934   **Figure supplement 1. Confirmation of βCBP binding to β-carotene via**
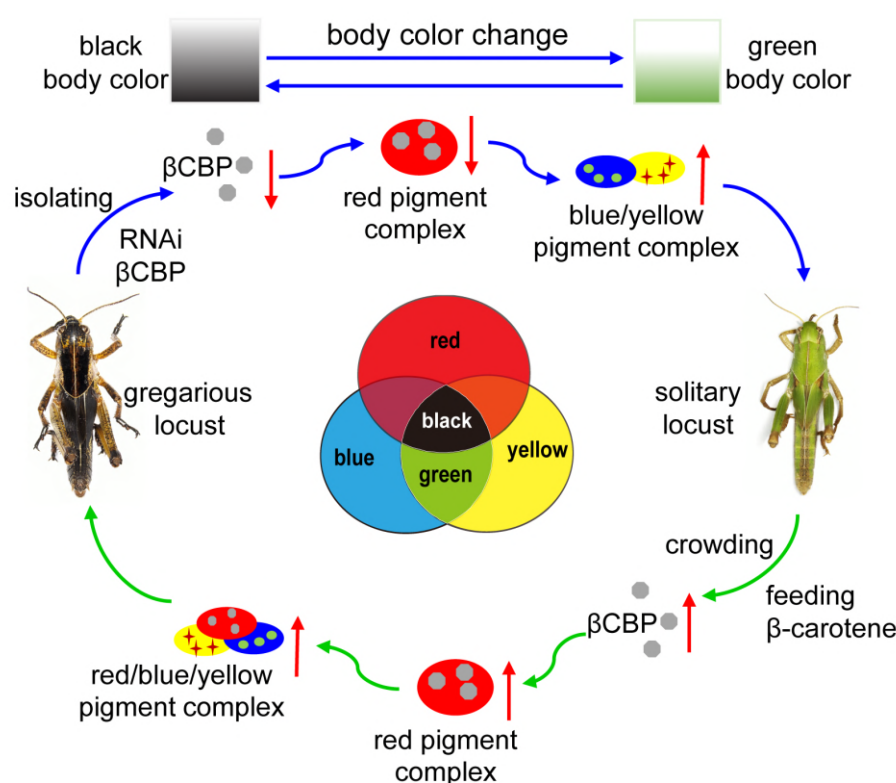
935   **HPLC.**

936

937

938

939

940

41

941

Figure 6. Model of a new mechanism in accordance with the physically trichromatic rule. Body color change is mediated by the red βCBP–β-carotene complex, which has a superposition effect on the solitary green background and produces the black back pattern of gregarious locusts. Silencing *βCBP* in gregarious locusts reduced the red color pigment β-carotene complex, thereby leading to the green pattern (instead of black). By contrast, feeding the solitary locusts β-carotene induced βCBP expression and caused gregarious-like body coloration.

The following figure supplement is available for figure 6:

Figure supplement 1. *Biliverdin-binding protein* and *carotene-binding protein* expression in the pronotum of gregarious and solitary locusts by qRT–PCR.**

954

Additional files

Supplementary files

Supplementary files 1. Primers used in the qPCR analysis of *βCBP*, and

***actin* and *GFP* used for RNA interference**

Supplementary files 2. Composition of the basic synthetic diet

960

961